PCCP

Accepted Manuscript

ROYAL SOCIETY OF CHEMISTRY

www.rsc.org/pccp

Cite this: DOI: 10.1039/c0xx00000x

www.rsc.org/xxxxxx

ARTICLE TYPE

Photoluminescence Tuning of $Na_{1-x}K_xNdW_2O_8$ ($0.0 \leq x \leq 0.7$) Nanoparticles; Synthesis, Crystal Structure and Raman Study

*Swetha S M Bhat[a], Ashfia Huq[b], Diptikant Swain[c], Chandrabhas Narayaan[c] and Nalini G Sundaram[a]**

Received (in XXX, XXX) Xth XXXXXXXXX 20XX, Accepted Xth XXXXXXXXX 20XX

DOI: 10.1039/b000000x

Series of $Na_{1-x}K_xNdW_2O_8$ ($0.0 \leq x \leq 0.7$) nanoparticles have been synthesized by an efficient glycothermal technique for the first time. SEM measurement confirmed the particle size ranges from 30-200 nm with ellipsoidal shaped morphology. Combined X-ray and neutron diffraction and Raman spectroscopy technique were utilized in order to investigate the influence of K^+ ion substitution in $NaNdW_2O_8$. K^+ ion substitution in the crystal lattice introduced change in Nd-O bond length and Nd-O-W bond angle of $NaNdW_2O_8$. The photoluminescence intensity increased up to the threshold composition x =0.4. K^+ ion substitution resulted in blue shifted emission of $NaNdW_2O_8$.Size mismatch, Nd-O-W angle and local disorder contributed to the observed difference in luminescence property. Also, chromaticity diagram for this blue emitting phosphor showed the possibility of tuning the emission by incorporation of K.

1. Introduction

Recently solid state lighting devices have become an alternative for conventional lighting sources due to their thermal stability, luminescence efficiency and their compact size.[1] At the same time solid state lighting devices emitting white light are drawing more attention in luminescence field due to their color purity. It is to be noted that the conventional method of obtaining white light is by the combination of blue LED InGaN chip and yellow emitting phosphors, YAG:Ce.[2] This methodology suffers from poor spectral distribution and color rendering property. Hence advanced techniques such as coating red, green and blue emitting phosphors on the UV LED chip is emerging[3] to obtain white light. However, this alternative trichromatic approach for new generation solid state lighting technology results in reduced photoluminescence.[4] Commercially available efficient blue emitting phosphor, $BaMgAl_{10}O_{17}:Eu^{2+5}$, despite showing high efficiency, experiences low thermal stability. Consequently, researchers are presently focusing on engineering materials with rare earth doped host phosphors which could be excited in the UV region and emit in visible region for efficient white light LED applications.[6] In this context, rare earth doped photoluminescent materials are extensively used for solid state lighting devices owing to efficient transition between f-f levels and d-f levels of rare earth ion.[7] Therefore, systems consisting of rare earth ions provide the possibility of tuning luminescence property ranging from UV, visible and IR regions, depending on host materials.

In addition to rare earth ions, materials comprising of alkali metal ions have also been utilized to alter the photoluminescence property by changing band width as well as intensity of the peak.[8] To improve the luminescence efficiency, alkali metal ions, which intermediate the energy transfer from host matrix to an activator ion, have been incorporated.[9] However, from the literature it has been found that role of each alkali metal ion varies in different host systems in achieving the desired photoluminescence property. To name a few, significant increase in the intensity of photoluminescence was achieved upon addition of Li in $Y_2O_3:Er^{3+}$ host matrix by tailoring local symmetry of the luminescing ion.[10] Also, in order to improve the emission intensity, alkali metal ions have been used as a charge compensator in several phosphors.[11-12] Performance of the phosphor was evaluated in different alkali metal ion and found that ionic radius has an important role in deciding the photoluminescence property. Therefore, depending on the host matrix, effect of alkali metal ion on the luminescence property varies. In $CaMoO_4:Eu^{3+}$, increase of ionic radius of alkali metal ion leads to increase in photoluminescence intensity.[13] Whereas in $CaIn_2O_4$, Na^+ exhibits maximum emission intensity and is attributed to less distortion of Na^+ ion compared to Li^+ and K^+ ions.[14] On the contrary, Li^+ ion is proved to be advantageous in getting highest quantum yield for $CaMoO_4:Yb^{3+}$ system compared to other alkali metal ions, due to distortion of MoO_4 and Yb polyhedra.[15] It is apparent from the above reports that the influence of alkali metal ion on photoluminescence behavior is not completely understood.

Currently rare earth tungstates are drawing more and more attention as luminescent materials due to their potential applications in LEDs, biomedicals and telecommunications etc. There are very few reports available focusing on the alkali metal ion influence in photoluminescence property of tungstate phosphor. Keto *et al* [8]studied the local structure of different alkali metal rare earth tungstates using pair distribution function technique and found that K^+ ion resulted in broadened and intense emission peak. Recently, we have also studied the photoluminescence behavior of the two polymorphs of $KNdW_2O_8$[16] and found that the difference in luminescence properties of these two polymorphs is due to the distortion in Nd-O polyhedra. So in order to better understand the role of alkali metal ion on the luminescing ion, it is necessary to investigate

alkali rare earth tungstates substituted with another alkali metal ion. Most of the tungstates are synthesized by conventional solid state method, solvothermal and solution combustion technique. Among all these methods, solvothermal technique is found to be advantageous in yielding smaller and homogenous particles at lower temperature.[17] It is of interest to note that, $NaNdW_2O_8$ has been investigated for laser applications and exhibits photoluminescence property in near IR region.[18] However to the best of our knowledge, K substituted $NaNdW_2O_8$ has not been investigated for visible light photoluminescent applications.

In this study, we present for the first time synthesis of $Na_{1-x}K_xNdW_2O_8$ ($0.0 \leq x \leq 0.7$) by an efficient glycothermal technique. Influence of K^+ ion substitution on the local environment of Nd polyhedra in $NaNdW_2O_8$ system has been studied by combined X-ray and neutron diffraction measurements. Raman study was performed to identify the existence of any local structure deviation in tungstate tetrahedra. Photoluminescence measurements and Chromaticity diagram reveals tuning of luminescence property of $NaNdW_2O_8$ by the addition of K^+ ion. This study demonstrates the possibility of engineering phosphor material into a promising candidate for solid state lighting devices with introduction of K^+ ion into Na^+ site of $NaNdW_2O_8$.

2. Experimental

Na_2CO_3, K_2CO_3, $Nd(NO_3)_3$ and $Na_2W_2O_4.H_2O$ have been used as starting materials. Stoichiometric amount of the reactants were added to 50ml of ethylene glycol solvent and stirred for 1h at room temperature to dissolve all reactants. The clear solution was poured to Teflon lined autoclave of 100 ml capacity. Autoclave was heated at 210^0C for 16h. The pink precipitate was separated from the solvent by centrifugation and washed with water and ethanol. Then the precipitate was dried at 97^0C

3. Characterization

Size and morphology of the synthesized particles were analyzed by field emission scanning electron microscopy using Carl Ziesses instrument. X-Ray powder diffraction data was collected for 8h with 0.02˚ step size for 2Θ range from 5 -90˚ on a Bruker D2 Phaser consisting of Cu Kα (λ= 1.5418Å) with a Lynx Eye positional detector.

Neutron time of flight powder diffraction data for all samples was collected at room temperature on POWGEN neutron diffractometer, at Spallation Neutron Source in Oak Ridge National Laboratory. Approximately 1g of each sample was filled in 8mm vanadium can and data was collected at 300K for d-spacing range from 1-4Å. Rietveld refinement was carried out using GSAS interface with EXPGUI.[19] Raman spectra was recorded in 180° back scattering geometry, using a 532 nm excitation from a diode pumped frequency doubled Nd:YAG solid state laser (model GDLM-5015 L, Photop Suwtech Inc., China) and a custom-built Raman spectrometer equipped with a SPEX TRIAX 550 monochromator and a liquid nitrogen cooled CCD (Spectrum One with CCD 3000 controller, ISA Jobin Yovn). Laser power at the sample was ≈ 8mW, and a typical spectral acquisition time was 1 min. The spectral resolution chosen was 2 cm^{-1}.

Photoluminescence property was investigated by PerkinElmer instrument with Xe lamp as a source.

4. Results and Discussion

4.1 Morphology

Morphological study was carried out using FE-SEM (Fig. 1 (a-e)).Spherical and elliptical like nanoparticles with size range from 40 to 200 nm are observed.

The plausible mechanism for formation of $Na_{1-x}K_xNdW_2O_8$ can be explained on the basis of previous reports on solvothermal synthesis of $NaLaW_2O_8$[20] and $NaYMo_2O_8$.[21] The solvent, in our case, ethylene glycol, proved to be a good complexing agent with cations for the synthesis of rare earth tungstates. As explained by Liu *et al*[21] growth mechanism follows dissolution, renucleation and Ostwald ripening to form nanoparticles. Once the cations dissolve in the solvent, they attack on WO_4^{2-} moiety to form nuclei of $Na_{1-x}K_xNdW_2O_8$. The formed nuclei slowly grow on smaller particles and evolve as nanoparticles to give thermodynamically favored shape and size. The evolution of elliptical shaped particles could be due to growth of nuclei along the direction of high surface energy.

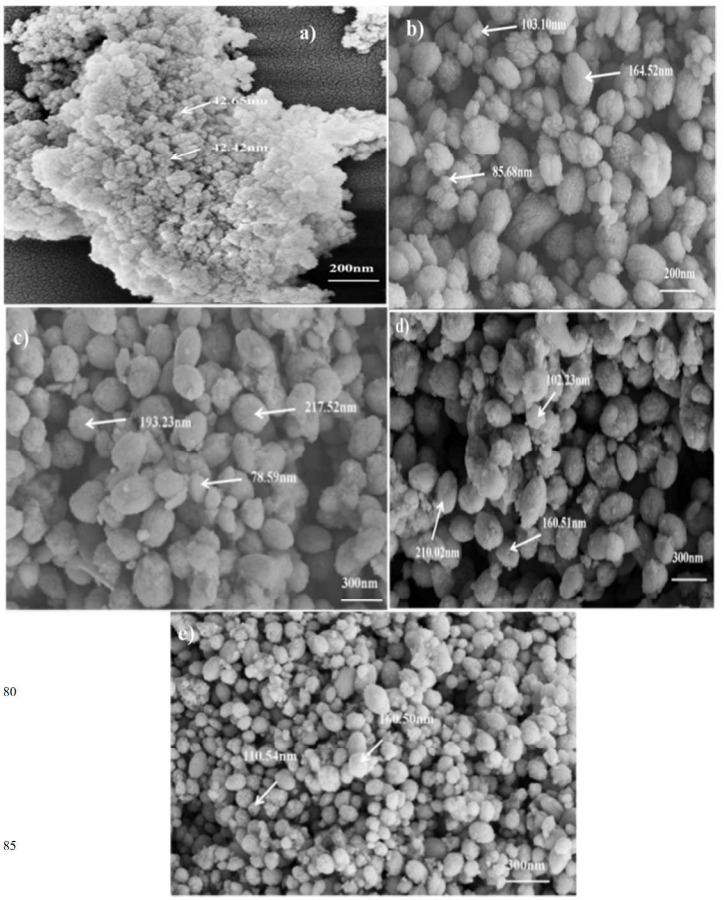

Fig.1 SEM images of $Na_{1-x}K_xNdW_2O_8$ a) x =0.0 b) x =0.2 c)x =0.4 d)x =0.6 e)x =0.7

Closer inspection of the SEM images reveals that, $NaNdW_2O_8$ yielded smaller, spherical shaped as well as homogeneous particles with an average size of 42 nm. However, K^+ ion substituted $NaNdW_2O_8$ samples i.e $Na_{1-x}K_xNdW_2O_8$ (x=0.2, 0.4, 0.6, 0.7) form bigger ellipsoids with sizes ranging from 80-200 nm. It is evident from the SEM images that incorporation of K^+ ion into $NaNdW_2O_8$ resulted in drastic change in morphology. Specifically, the smaller nearly spherical shaped nanoparticles which are agglomerated in $NaNdW_2O_8$ undergo morphological transformation to give ellipsoid nanoparticles with size 80-200 nm. This difference in size and morphology can be explained based on Dong *et al*'s[22] observations in $NaGd_{1-x}Yb_xF_4$ systems. According to their study change in morphology is due to variations in surface electron charge density caused when an ion with different ionic radius is substituted. Extrapolating this observation, we believe that, when larger K^+ ion is substituted in smaller Na^+ ion site, the obvious increase in surface electron charge density modifies the morphology of the particle. Once the electron charge density varies, dipole polarizibility could also be altered. Consequently, K^+ ion in lattice influences on the nucleation of smaller particles resulting in thermodynamically stable mono dispersed ellipsoidal particles. It is observed that upon increase in the K^+ ion content i.e from x=0.2 to 0.7, the ellipsoidal nanoparticles are retained without any further size and morphology modification. It can be surmised from the above observations that K^+ ion substitution promotes morphological change in $NaNdW_2O_8$.

Additionally, the above results indicate that this template free glycothermal method is a very versatile technique which can be used to achieve different morphologies for tungstate materials. In this case, size and shape of $NaNdW_2O_8$ can be tuned with the substitution of K^+ ion.

4.2. Combined X-Ray and neutron diffraction study

4.2.1 X-ray powder diffraction (XPD) study

Prior to the neutron experiment, phase was confirmed from laboratory XPD which was collected for all samples. All data match with ICSD nu 66091 except the reflection at 2Θ=25.3° which corresponds to a minute amount of Nd_2WO_6 in the material. All $Na_{1-x}K_xNdW_2O_8$ ($0.0 \leq x \leq 0.7$) samples crystallize in tetragonal phase with centrosymmetric space group $I4_1/a$. Fig. 2 represents the XPD patterns for all samples. As expected, after K incorporation, shift towards lower angle in the powder pattern was observed due to the expansion of unit cell (Fig.3). Rietveld refinement was carried out for all the samples using GSAS suite interfaced with EXPGUI. The background was refined using shifted Chybeshev polynomial function. Diffraction profile for all data was fitted by pseudo-Voigt function. All cations in the structure were present in special position. The position of oxygen atoms were refined keeping occupancy and thermal parameter fixed. Since, K, Na and Nd atoms occupy the same crystallographic site with Wyckoff position 4a, thermal parameter and occupancy of Na, K and Nd atoms were refined alternatively. Observed and difference plot obtained from Rietveld refinements are represented in Fig 4.

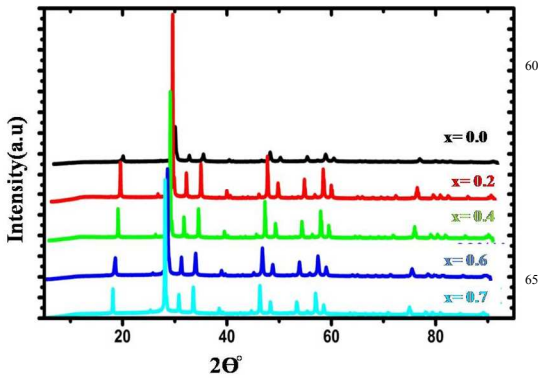

Fig.2 XPD pattern for $Na_{1-x}K_xNdW_2O_8$

4.2.2 Neutron powder diffraction (NPD) study

Neutron diffraction study is essential in order to accurately measure the positions of light atoms in presence of heavy elements. Even though, crystal structure could be refined from X-ray diffraction, neutron diffraction data is necessary when host matrix consists of lighter oxygen atoms. Since neutron sees scattering length of oxygen with ease, ambiguity in determining positions of oxygen can be overcome from NPD experiment. However, since K and Na have very similar coherent scattering length, occupancy refinements were carried out using X-ray diffraction data. Subsequently, oxygen positions obtained from NPD were utilized in X-ray Rietveld refinement.

Fig.5 represents observed, calculated and difference plots obtained from Rietveld refinement. Crystallographic parameters obtained from combined XPD and NPD are listed in Table 1.

It is evident from the table that lattice parameters and hence the volume of unit cell has expanded with increase in the concentration of K^+ ion in the unit cell. This can be attributed to the higher ionic radius of K^+ ion (1.51Å) compared to that of Na^+ ion (1.18Å). Surprisingly, above x=0.4, there is only a marginal expansion of unit cell parameter (Fig.6). This indicates that K^+ ion substitution in $NaNdW_2O_8$ reaches an optimum concentration after which, no consistent expansion of unit cell parameters have

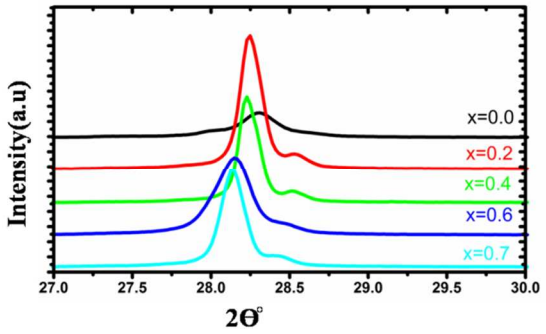

Fig.3 XPD pattern from 27° to 30° for $Na_{1-x}K_xNdW_2O_8$ indicating lattice expansion

been observed. It is noteworthy that $Na_{1-x}K_xNdW_2O_8$ retains parental crystal system i.e tetragonal symmetry even after increase in concentration of K^+ ion. The end compound $KNdW_2O_8$[16] is known to exist in tetragonal phase and hence retention of tetragonal crystal system for $Na_{1-x}K_xNdW_2O_8$ is possible. Atomic co-ordinates and occupancy are represented in Table 2. Fig.7 represents the crystal structure of $Na_{1-x}K_xNdW_2O_8$ along 'b' direction. Na, K and Nd atoms occupy same crystallographic special position (Wyckoff site 4a). The tungsten atom also sits in a special position (Wyckoff site 4b) whereas oxygen atom is in general position (16f Wyckoff site). K, Na and Nd are surrounded by eight oxygen atoms forming polyhedra with two different bond lengths. Nd/K/Na-O polyhedra are edge shared and built in a chain along *'ac'* plane. Tungsten forms regular tetrahedra which are connected to each other through oxygen atoms and shared with Nd-O polyhedra. Bond lengths and angles obtained from Rietveld refinement for all compositions are listed in Tables 3 and 4. Since the local environment of Nd^{3+} ion mainly decides the photoluminescent behaviour, minor changes in bond length and bond angles play major role in any change in the photoluminescent property. It is clear from the Table 3 and 4 that inclusion of K^+ ion in the lattice leads to difference in bond lengths and angles between the luminescing neodymium and oxygen ions. Fig.8 depicts the Nd-O-W bond angle for all samples.

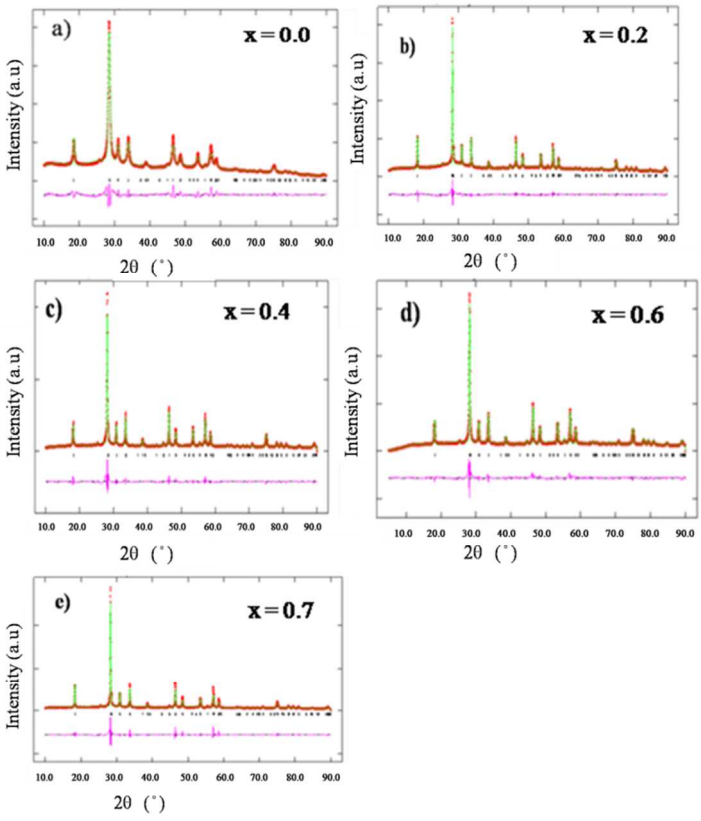

Fig.4 Difference plot obtained from Rietveld refinement of X-ray diffraction data for a) $NaNdW_2O_8$ b)$Na_{0.8}K_{0.2}NdW_2O_8$ c)$Na_{0.6}K_{0.4}NdW_2O_8$ d) $Na_{0.4}K_{0.6}NdW_2O_8$ e) $Na_{0.3}K_{0.7}NdW_2O_8$

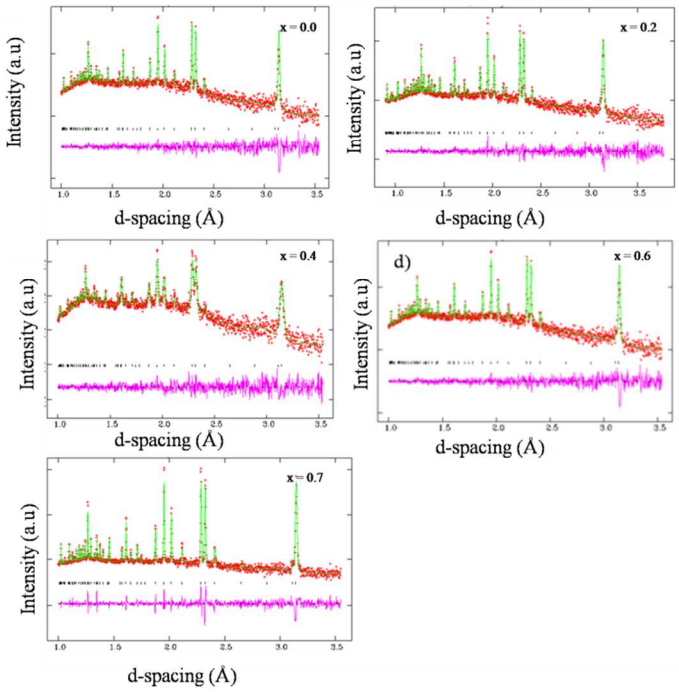

Fig.5 Difference plot obtained from Rietveld refinement of neutron diffraction data for a) $NaNdW_2O_8$ b)$Na_{0.8}K_{0.2}NdW_2O_8$ c)$Na_{0.6}K_{0.4}NdW_2O_8$ d) $Na_{0.4}K_{0.6}NdW_2O_8$ e) $Na_{0.3}K_{0.7}NdW_2O_8$

From Table 3 it can also be deduced that the average bond length is highest for x = 0.4, further it decreases with addition of K^+ ion. This suggests that x = 0.4 is a threshold composition beyond which any further increase in K^+ ion content has no effect in increasing Nd-O bond length. The optimum angle between activator ion and intervening oxygen ligand plays a crucial role since it predicts extent of interaction of *p*-orbital of oxygen ion.[23] Table 4 shows selected bond angles between Nd-O-W responsible for energy transfer from host matrix to luminescing ion (Nd^{3+}). Maximum energy transfer is possible if the angle is near to 180° via linear p-orbital of oxygen ions.[23] It has been reported in literature that for $KEuW_2O_8$ system, the maximum angle for W-O-Eu found to be 176° which yields maximum photoluminescence intensity compared to $NaEuW_2O_8$

Table 1.Crystallographic data obtained from Rietveld refinement of combined X-ray and neutron diffraction data

	a) $NaNdW_2O_8$	b)$Na_{0.8}K_{0.2}NdW_2O_8$	c)$Na_{0.6}K_{0.4}NdW_2O_8$	d) $Na_{0.4}K_{0.6}NdW_2O_8$	e) $Na_{0.30}K_{0.7}NdW_2O_8$
Space Group	$I4_1/a$	$I4_1/a$	$I4_1/a$	$I4_1/a$	$I4_1/a$
a (Å)	5.278(4)	5.298(1)	5.301(1)	5.302(1)	5.300(1)
b (Å)	5.278(4)	5.298(1)	5.301(1)	5.302(1)	5.300(1)
c (Å)	11.505(2)	11.480(1)	11.512(1)	11.519(1)	11.533(1)
Volume of unit cell ($Å^3$)	320.56(4)	322.20(1)	323.55(1)	323.77(1)	323.99(1)
R_{wp}(%)	10.07	8.22	11.20	9.42	10.85
R_p (%)	7.89	6.3	8.8	7.47	8.56
R(I,hkl)(%)	8.24	10.73	7.9	9.35	8.75

Table 2.Oxygen positions* of $Na_{1-x}K_xNdW_2O_8$ and Occupancy of K,Na and Nd

	Oxygen positions			Occupancy		
Samples	**x**	**y**	**z**	**Na**	**K**	**Nd**
$NaNdW_2O_8$	**0.798(1)**	**0.622(1)**	**0.033(1)**	**0.49(1)**	**-**	**0.51(1)**
$Na_{0.8}K_{0.2}NdW_2O_8$	**0.753(1)**	**0.604(1)**	**0.043(1)**	**0.41(1)**	**0.08(1)**	**0.51(1)**
$Na_{0.6}K_{0.4}NdW_2O_8$	**0.735(1)**	**0.615(1)**	**0.042(1)**	**0.30(1)**	**0.21(1)**	**0.49(1**
$Na_{0.2}K_{0.6}NdW_2O_8$	**0.738(1)**	**0.602(1)**	**0.042(1)**	**0.17(1)**	**0.33(1)**	**0.51 (1)**
$Na_{0.3}K_{0.7}NdW_2O_8$	**0.751(1)**	**0.603(1)**	**0.041(1)**	**0.14(1)**	**0.36(1)**	**0.49(1)**

***Na,K,Nd at (0.0 0.75 0.875) and W at (0.5 0.75 0.125)**

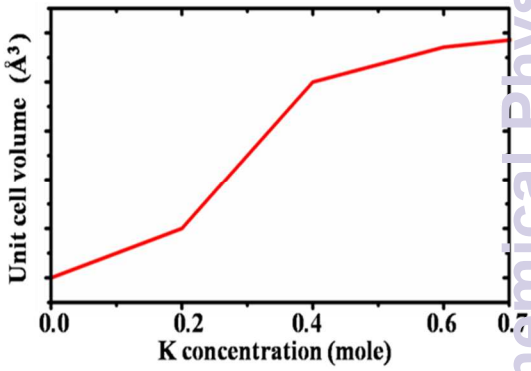

Fig.6 Unit cell expansion of $Na_{1-x}K_xNdW_2O_8$ as a function of K concentration

Table 3.Selected bond distances of $Na_{1-x}K_xNdW_2O_8$

Bond type	CN	a) $NaNdW_2O_8$ Bond length (Å)	b)$Na_{0.8}K_{0.2}NdW_2O_8$ Bond length (Å)	c)$Na_{0.6}K_{0.4}NdW_2O_8$ Bond length (Å)	d) $Na_{0.4}K_{0.6}NdW_2O_8$ Bond length (Å)	e) $Na_{0.3}K_{0.7}NdW_2O_8$ Bond length (Å)
K/Na/Nd -O	4	2.40(1)	2.46(1)	2.49(1)	2.50(1)	2.44(1)
Na/K/Nd-O	4	2.43(1)	2.47(1)	2.58(1)	2.51(1)	2.52(1)
W-O	4	1.88(1)	1.81(1)	1.72(1)	1.77(1)	1.81(1)

Table 4.Selected bond angles of $Na_{1-x}K_xNdW_2O_8$

Angle type	a) $NaNdW_2O_8$ Bond Angle(˚)	b)$Na_{0.8}K_{0.2}NdW_2O_8$ Bond Angle (˚)	c)$Na_{0.6}K_{0.4}NdW_2O_8$ Bond Angle(˚)	d) $Na_{0.4}K_{0.6}NdW_2O_8$ Bond Angle(˚)	e) $Na_{0.3}K_{0.7}NdW_2O_8$ Bond Angle(˚)
Nd-O-W	129.57(1)	131.80(1)	135.79(1)	132.33(1)	131.99(1)

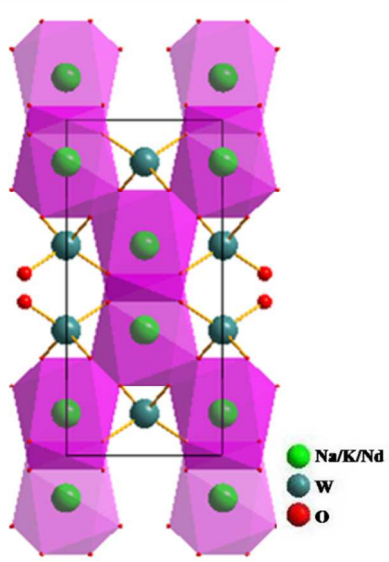

Fig.7 Unit cell representation of $Na_{1-x}K_xNdW_2O_8$ along b direction

and $LiEuW_2O_8$ which is near to 143°.[8] In the present case, as amount of K^+ ion increases in the lattice of $NaNdW_2O_8$, bond angle also increases up to x = 0.4 and decreases by a trivial amount for x= 0.6 x = 0.7. Therefore, it is appropriate to infer that, since x= 0.4 in the host matrix has highest W-O-Nd bond angle; it is expected to exhibit high photoluminescence intensity.

Raman Study

It is well known that Raman spectroscopy is an excellent tool for capturing the structural changes in terms of vibrational frequencies while an external atom is substituted in the host matrix. Raman spectra were collected in order to verify if the local structure remains unaffected with substitution of K^+ ion in host matrix. Fig.9 represents Raman spectra of $Na_{1-x}K_xNdW_2O_8$ ($0.0 \leq x \leq 0.7$) collected in the frequency range 100-1000 cm^{-1} and at 298K. All the Raman active modes were assigned based on information available in literature[24] .The normal mode analysis of a free tetrahedral WO_4^{-2} ion predicts its fundamental vibrational frequencies at ν_1 (A_1):928, ν_2 (E):320, ν_3 (F_2):833, ν_4(F_2):405 cm^{-1}, where ν_1: the symmetric stretching mode, ν_2: the doubly degenerate symmetric bending mode, ν_3: the triply degenerate asymmetric stretching mode, and ν_4: the triply degenerate asymmetric bending mode. However, when the symmetry of WO_4^{-2} in the crystalline environment lowers, band positions will shift and also split. Generally, in the solid state, isolated tetrahedra show stretching modes in the range 750-1000 cm^{-1} and bending modes in the range 250-430 cm^{-1}, whereas the translational and librational modes appear below 250 cm^{-1}. It can be confirmed that addition of K^+ ion in the lattice does not change local structure or symmetry of these compounds as we do not see any significant change in the Raman spectra. However a little softening of stretching frequency observed around 920 cm^{-1} could be attributed to insertion of K^+ ion in the lattice.

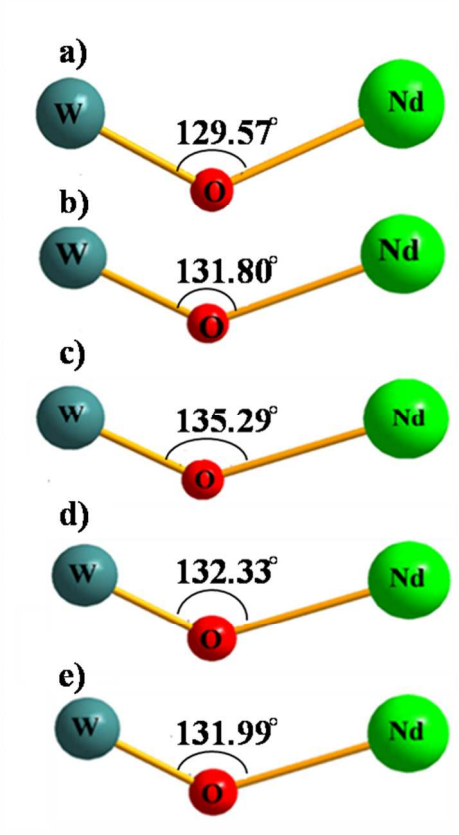

Fig.8 Nd-O-W angle for $Na_{1-x}K_xNdW_2O_8$ where a) x =0.0, b) x = 0.2, c) x = 0.4, d) x = 0.6, e) x = 0.7

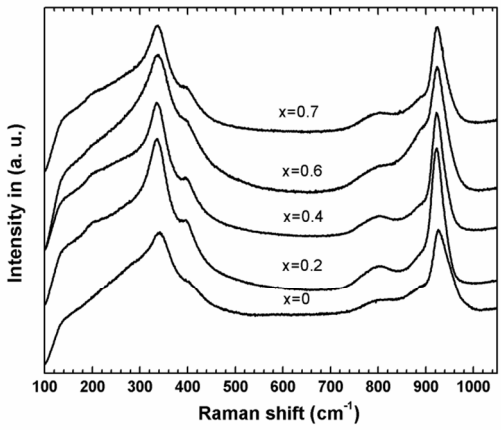

Fig.9 Raman shift for $Na_{1-x}K_xNdW_2O_8$

4.4 Photoluminescent behaviour

Fig.10 represents the photoluminescence excitation spectra recorded at 440 nm emission wavelength for all samples. Excitation spectrum show broad band from 320 to 420 nm. This implies that these materials can be efficiently excited from near UV to blue regions of the visible light. Excitation ranges from 320- 420 nm are characteristic f-f level transition of Nd^{3+} ion. The excitation corresponds to the transition from $^4I_{9/2}$-$^4D_{5/2}$, $^2P_{1/2}$ of luminescing Nd^{3+} ion.

Photoluminescence emission spectra monitored at 390 nm excitation wavelength (Fig.11) show broad emission band which originates from 400 nm and ends at 525 nm covering entire blue and green region (Fig.11). The strongest emission peaks are centred in between 440- 450 nm for all samples. It is evident from emission spectra that, introduction of K^+ ion in to Na^+ ion site changes the photoluminescence spectra significantly. Peak situated at 440 nm is assigned to $^3P_{1/2}$+$^4D_{5/2}$- $^4I_{9/2}$ and at 480 nm emission corresponds to $^4I_{9/2}$-$^4G_{9/2}$+$^4D_{3/2}$+$^4G_{9/2}$+ $^4K_{15/2}$ transition.[25] As the amount of K^+ ion increases, luminescence intensity also increases up to x= 0.4 after which it decreases (Fig.12). It is also noticed that with increase in concentration of K, a blue shift is observed for the transition corresponding to $^4I_{9/2}$-$^2P_{1/2}$.

Even though, K^+ ion substitution has not contributed to any remarkable change in crystal symmetry, it has significant influence on the photoluminescence property. Accommodating three cations Na^+, K^+ and Nd^{3+} with different ionic radius in the same crystallographic site can lead to considerable change in the photoluminescence property of materials. From the emission spectra it is evident that there is a pronounced blue shift with substitution of K^+ ion. This can be explained on the basis of difference in sizes of cation; Na and K with ionic radius 1.18 and 1.51Å occupy the Nd (1.29Å) site. It has been reported in literature that there is a direct dependency of energy shift with size mismatch of the cation.[26] As the size difference between luminescing ion and alkali cation increases, energy shift towards shorter wavelength is observed. As K^+ ion occupies the Na site, difference in size i.e $\Delta r = r(M^+) - r(Nd^{3+})$ increases, hence we presume that this size difference resulted in blue

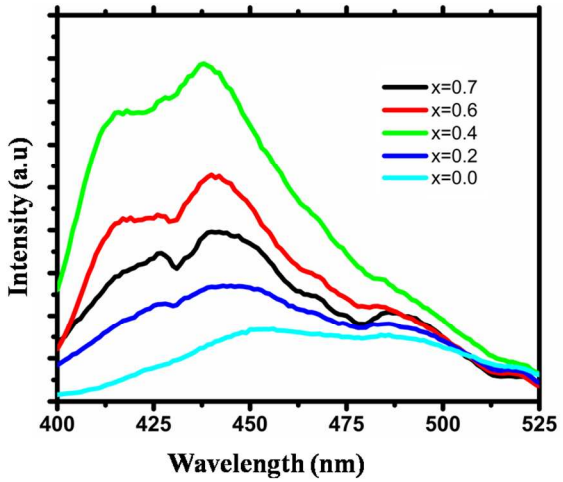

Fig.11 Emission spectra monitored at 390nm excitation wavelength for $Na_{1-x}K_xNdW_2O_8$

shift in the photoluminescence peaks.

The inhomogeneous broadening of spectral lines observed for all compositions can be correlated to the local disorder in the cation sites. As $Na_{1-x}K_xNdW_2O_8$ series crystallize in centrosymmetric $I4_1/a$ space group, cations K^+, Na^+ and Nd^{3+} occupy the same crystallographic site with the Wyckoff position 4a. It well known that systems exhibiting this type of local disorder, usually contribute to the observed bandwidth of the photoluminescence peak.[27]

There are several factors that contribute to the increasing intensity of the photoluminescence peak on K^+ ion substitution, the obvious reason being the incorporation of K^+ ion into Na lattice. It is reported that introduction of alkali metal ion disturbs the bound electron-hole pair. [9] As explained by J. Li *et al*[9] as the alkali metal ion is introduced in the lattice, difference in ionic radius increases, resulting in increase of population of electrons and holes in conduction band and valence band respectively. This phenomenon progressively facilitates electron hole recombination to occur. Therefore, probability to capture holes present in the

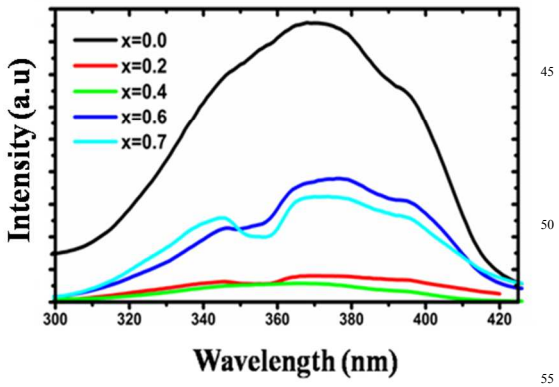

Fig.10 Excitation spectra monitored at 440nm emission wavelength $Na_{1-x}K_xNdW_2O_8$

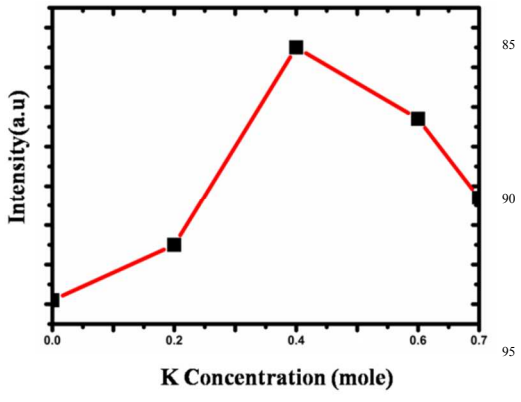

Fig.12 emission intensity vs K concentration for $Na_{1-x}K_xNdW_2O_8$

ground state and electron in the excited state increases for Nd^{3+} ion which eventually lead to enhanced intensity in the photoluminescence. It can be noticed from the spectra that as concentration of K^+ ion increases, photoluminescence intensity increases up to x = 0.4. We believe that further increase in K^+ ion content could lead to defect in the system and eventually decreases luminosity. This implies that the appropriate concentration to achieve maximum intensity, for $NaNdW_2O_8$ is 40% of K^+ ion.

Increased intensity of photoluminescence peak can also be explained on the basis of crystal field strength and optimum angle between Nd-O-W. It has been noticed in many reports[28,8,16] that bond distance between rare earth and oxygen ion influence the photoluminescence intensity and structure of emission band. Table 3 shows that as K^+ ion concentration increases in the lattice, ionic radius increases and Nd-O distance also increases. It is well known that crystal field strength decreases as Nd-O bond distance increases. However we observe that with increasing Nd-O bond distances from x=0 to 0.4, there is enhancement in the photoluminescence peak intensity, after which it decreases. This phenomenon can be explained on the basis of optimum angle in W-O-Nd for efficient energy transfer.[23] It has been reported in literature that energy exchange through intervening oxygen increases and is optimum near to 180° angle.[23] It can be seen from table 4 that the W-O-Nd bond angle increases up to 0.4 as a function of K^+ ion concentration. The maximum bond angle of 135.29° obtained for x = 0.4 exhibits most intense emission peak than any other compositions.

4.5 Chromaticity Study

Chromaticity diagram demonstrates the colour response for $Na_{1-x}K_xNdW_2O_8$ series in CIE 1931 chromatic diagram for 2° observer. Fig.13 shows chromaticity co-ordinates for all the samples.

Colour of $NaNdW_2O_8$ can be tuned from blue to violet blue by disturbing the local environment of Nd polyhedra via introduction of K^+ ion. Table.5 lists the colour co-ordinates for all samples which are excited at 390 nm. Color dots in the CIE diagram indicate colour co-ordinates. $NaNdW_2O_8$ colour co-ordinates are situated at (0.18, 0.21), a blue region can be tuned to (0.17, 0.15), (0.16, 0.11) and eventually yields (0.16, 0.08), a blue emitting phosphor with increase in the substitution of K^+ ion. It is evident from the chromaticity diagram that, x =0.4 sample emits in violet blue region and is suitable for near UV emitting phosphor applications. This detailed crystal structure-photoluminescence study correlates the effect of alkali metal ion (K^+) substitution in Na^+ site with the photoluminescence property.

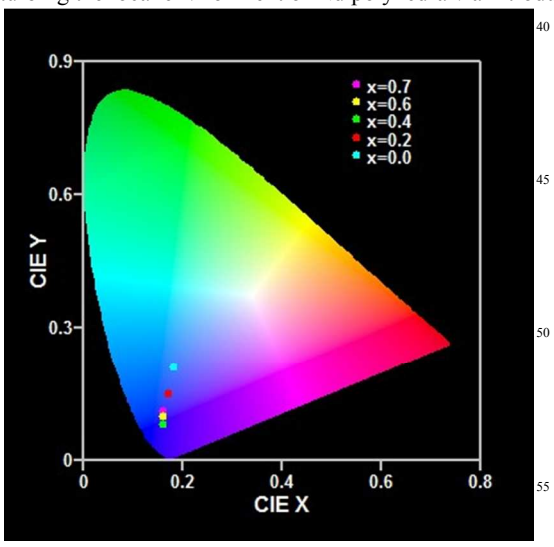

Fig. 13 Chromaticity diagram for $Na_{1-x}K_xNdW_2O_8$

Table 5. Color co-ordinates

Samples	Colour co-ordinates	
	x	y
$NaNdW_2O_8$	0.18	0.21
$Na_{0.8}K_{0.2}NdW_2O_8$	0.17	0.15
$Na_{0.6}K_{0.4}NdW_2O_8$	0.16	0.08
$Na_{0.4}K_{0.6}NdW_2O_8$	0.16	0.10
$Na_{0.2}K_{0.8}NdW_2O_8$	0.16	0.11

5. Conclusion

$Na_{1-x}K_xNdW_2O_8$ (0.0≤ x ≤0.7) nanoparticles have been successfully synthesized by glycothermal method for the first time. Spherical and ellipsoidal shaped particles with the size range 30-200 nm was obtained from glycothermal technique. Rietveld refinement carried over combined X-ray and neutron powder diffraction shows incorporation of K^+ at Na^+ site causes expansion of lattice parameter. Raman study verifies that the local structure and symmetry of the compounds are unaffected by K^+ substitution. However, K^+ ion substitution resulted in significant changes in Nd-O bond length and Nd-O-W bond angle even though they retain parental crystal symmetry. $Na_{1-x}K_xNdW_2O_8$ (0.0≤ x ≤0.7) exhibit blue luminescence and can be tuned with incorporation of K^+ ion. Emission spectra are blue shifted with increment of K^+ ion concentration. The intensity of photoluminescence increases up to an optimum value of x = 0.4 and further increase in K^+ ion results in decreased intensity. Observed blue shift is due to the size difference of K^+ and Na^+ ions. Local occupancy disorder in the centrosymmetric $I4_1/a$ space group contributed to the broadness of luminescence spectra. The enhanced intensity of the photoluminescence attributed to increase in Nd-O-W bond angle which facilitates efficient energy transfer. Chromaticity coordinates can be varied from (0.18, 0.21) to (0.16, 0.08) for $Na_{1-x}K_xNdW_2O_8$ (0.0≤ x ≤0.7), showing x=0.4 is the threshold composition for K concentration. $Na_{1-x}K_xNdW_2O_8$ (0.0≤ x ≤0.7) phosphor is a potential candidate for blue light emitting devices which can be further exploited for the production of white light LEDs. This study unequivocally establishes influence of alkali metal ion on the shift and emission intensity of photoluminescence property in this class of materials.

Acknowledgements

Swetha S M thanks UGC, India for the fellowship and Manipal University, India for accepting this work as part of PhD program**.** Swetha S M Bhat and Nalini G Sundaram thank Joydeep and Satish Patil SSCU, IISc, Bengaluru for photoluminescence facility. A portion of this research at ORNL's Spallation Neutron Source, was sponsored by the Scientific User Facilities Division, Office of Basic Energy Sciences, U.S. Department of Energy

Affiliations

a.Materials Science Division, Poornaprajna Institute of Scientific Research(PPISR), Bidalur post, Devanahalli, Bengaluru-562110, India.

b.Chemical and Engineering Materials Division Spallation Neutron Source, Oak Ridge National Laboratory, Tennessee 37831, United States.

c.CPMU, Jawaharlal Nehru Centre for Advanced Scientific Research, Jakkur, Bengaluru, India

E-mail:nalini@poornaprajna.org;Fax:+9123611836;Tel: +9127408552

References

1. E. F. Schubert and J. K. Kim, *Science*, 2005, 308, 1274-1278.
2. L. Chen, C.C. Lin, C.W. Yeh and R.S. Liu, *Mater.*, 2010, 3, 2172-2195.
3. J. K. Sheu, S. J. Chang, C. H. Kuo and Y. K. Su, *IEEE Photonic.Tech L*, 2003, 15, 18-20
4. S. Neeraj, N. Kijima and A. K. Cheetham, *Chem.Phys.Lett.*, 2004, 387, 2-6.
5. P. Zhu, Q. Zhu, H. Zhu, H. Zhao, B. Chen, Y. Zhang, X. Wang and W. Di, *Opt.Mater.*, 2008, 30, 930-934.
6. Y. Zhou and B. Yan, *CrystEngComm*, 2013, 15, 5694.
7. M. Nazarov and D .Y.Noh, *J.Rare Earth*, 2010, 28, 1-11.
8. J. Huang, J. Xu, H. Luo, X. Yu and Y. Li, *Inorg. Chem*, 2011, 50, 11487-11492.
9. J. Li, Y. Wang and B. Liu, *J. Lumin.*, 2010, 130, 981-985.
10. T. Fan, Q. Zhang and Z. Jiang, *J. Opt.*, 2011, 13, 015001.
11. J. Liu, H. Lian and C. Shi, *Opt. Mater.*, 2007, 29, 1591-1594.
12. G. Li, T. Long, Y. Song, G. Gao, J. Xu, B. An, S. Gan and G. Hong, *J. Rare Earth.,* 2010, 28, 22-25.
13. S. Shi, J. Gao and J. Zhou, *Opt. Mater.*, 2008, 30, 1616-1620.
14. X. Yan, W. Li and K. Sun, *J. Alloys Compd*, 2010, 508, 475-479.
15. X. Cao, T. Wei, Y. Chen, M. Yin, C. Guo and W. Zhang, *J. Rare Earths*, 2011, 29, 1029-1035.
16. S. S. M. Bhat, D. Swain, C. Narayana, M. Feygenson, J. C. Neuefeind and N. G. Sundaram, *Cryst.Growth Des.*, 2014, 14, 835-843.
17. D.R.Modeshia and R. I. Walton., *Chem. Soc. Rev*., 2010, 39, 4303–4325
18. A. Kato, N. Uchitomi, S. Oishi, T. Shishido and S. Iida, *Phys.Status Solidi (c)*, 2006, 3, 2709-2712.
19. A. C. L. a. R. B. V. Dreele, *General Structure Analysis System (GSAS)*, Los Alamos National Laboratory, 2004.
20. X. Liu, W. Hou, X. Yang and Q. Shen, *Dalt. Trans.,* 2013, 42, 11445-11454.
21. J.Liu,B.Xu,C.Song,H.Luo,X.Zou,L.Han and X.Y *CrystEngComm*, 2012, 14, 2936-2943
22. G. Dong,B.Chen,X.Xiao,G.Chai,Q. Liang M. Peng and J.Qiu *Nano Scale*. 2012, 4, 4658–4666
23. L. G. Van Uitert, R. C. Linares, R. R. Soden and A. A. Ballman, *J. Chem. Phys.,* 1962, 36, 702.
24. B. A. Kolesov and L. P. Kozeeva, *J. Struct. Chem.* 1993, 34, 534-539
25. F. B. A. Brenier, G. Metrat, N. Muhlstein, M. Boudeulle and G. Boulon, *J.Lumin*., 1999, 81, 135-141
26. W. T. Chen, H. S. Sheu, R. S. Liu and J. P. Attfield, *J.Am. Chem. Soc.*, 2012, 134, 8022-8025.
27. C. Colon, A. Alonso Medina, F. Fernandez, C. Cascales, R. Puche and C. Zaldo, *Chem. Mater. 2005, , 6635-6643*, 2005, 17, 6635-6643.
28. G.H. Lee, T.H. Kim, C.Yoon and S. Kang, *J.Lumin.*, 2008, 128, 1922-1926.